Available online at www.sciencedirect.com
SCIENCE DIRECT®
Catalysis Today 96 (2004) 79–89
CATALYSIS TODAY
www.elsevier.com/locate/cattod

NO_X storage and reduction on a Pt/BaO/alumina monolithic storage catalyst

Karen S. Kabin, Rachel L. Muncrief, Michael P. Harold*

Department of Chemical Engineering, University of Houston, S222 Engineering Bldg. 1, Houston, TX 77204-4004, USA

Available online 13 July 2004

Abstract

The performance of a $Pt/BaO/Al_2O_3$ washcoated monolith reactor is investigated using propylene as a reductant. The dependence of the time-averaged NO_X conversion is reported for several operating parameters, including feed composition, temperature, flow rate, propylene pulse duration and overall cycle time. NO_X storage data, which reveal both kinetic and thermodynamic limitations, provide guidance on selecting the feed protocol giving high NO_X conversion. Complex nonisothermal transient features spanning the NO_X storage and reduction regimes are revealed. Time-averaged NO_X conversions exceeding 80% are achieved over a wide range of feed temperatures when short pulses are fed that have a sufficiently high propylene concentration to create fuel-rich conditions. The periodic feed of propylene gives time-averaged NO_X conversion significantly exceeding the steady-state conversion for an equivalent propylene feed rate. The results indicate that the rich–lean feed protocol must be tuned in order to achieve a maximum NO_X conversion with minimal breakthrough of incompletely oxidized components. The time-averaged conversion achieves a maximum at an intermediate cycle time and reductant pulse duty, with values dependent on the feed temperature and flow rate. The results are compared to previous literature data and interpreted with a phenomenological storage and reduction cycle.

Keywords: NO_X; Diesel; Emissions; Catalysis; Reaction engineering; NO_X trap; NO_X storage and reduction; Monolith reactor

1. Introduction

Diesel-powered engines have better fuel economy than stoichiometric gasoline engines [1–6]. However, diesel engine exhaust has many adverse environmental effects, due to the emission of nitrogen oxides (NO_X), particulate matter (PM) and SO_2. There is an urgent need to develop diesel emission control technology to take full advantage of the fuel efficiency and durability of diesel vehicles. Emission standards for heavy-duty diesel vehicles in 2007 and beyond will require a 90% reduction in total particulate matter and NO_X from 2003 levels [7]. These standards place new demands on improved engine performance and catalytic converter technology.

The lean-burn conditions of diesel combustion, which yield a higher combustion temperature and improved efficiency, produce an exhaust containing an excess of oxygen. This complicates conventional approaches to chemically reduce NO_X. Considerable research and development efforts have been carried out in the last 10 years on diesel/lean-burn exhaust abatement of NO_X. Current NO_X reduction technologies include exhaust gas recirculation (EGR); selective catalytic reduction (SCR) utilizing anhydrous ammonia or aqueous urea injection [3,8,9]; direct decomposition of NO with Cu/zeolite catalyst [10]; steady-state selective catalytic reduction with hydrocarbons (HC-SCR) under lean conditions [10]; and periodic HC-SCR using a NO_X storage and reduction (NSR) catalyst. Previous NSR studies were reviewed in a previous publication [11]. NSR has been shown to be an effective approach for achieving high NO_X conversion for a lean feed. While many advances have been made with NO_X storage and reduction, there are obstacles towards its widespread deployment in lean-burn diesel vehicles. Salient issues were reviewed in a previous publication [11].

Many research studies have focused on powder catalysts, but monolith supports are used on vehicles. Here we review studies of NSR employing monoliths. Fridell et al. determined the NO_X storage capacity of model NSR mono-

* Corresponding author.
E-mail address: mharold@uh.edu (M.P. Harold).

0920-5861/$ – see front matter © 2004 Elsevier B.V. All rights reserved.
doi:10.1016/j.cattod.2004.05.008

lith catalysts as a function of temperature, O_2, CO_2, and reductant concentrations [12,13]. Amberntsson et al. [14] examined the influence of O_2 and CO_2 on the NO_X release step. They found that O_2 inhibits NO_X release by raising the desorption temperature while CO_2 promotes NO_X release by forming $Ba(CO_3)$. Theis et al. [15], in a comprehensive study, quantified the (unconverted) NO_X released from the lean NO_X trap during the rich purge. They showed that NO_X release was minimized when shorter lean periods were used (reducing the amount of NO_X stored) and when very rich purges were fed (providing excess reductant). They proposed that the exotherm created by the combustion of the reductant lowers the storage capacity and effects a release of NO_X [15]. Other groups have focused on the development and testing of kinetic models for monoliths in order to explain the storage and regeneration steps that occur during the NO_X trap process [16,17].

The current study is a comprehensive analysis of the performance of a model Pt/BaO/alumina washcoated monolith catalyst for NO_X storage and reduction. The study builds on the several previous studies that have reported high NO_X conversions during NO_X storage and reduction [11,15,18–21]. We examine the effects of several key operating variables on the time-averaged NO_X and propylene conversion, and NO_X to N_2 selectivity. In addition, we determine the reductant (propylene) feed protocol needed to achieve high NO_X conversion.

2. Experimental description

The samples used for these experiments were monolith catalysts provided by Engelhard Corporation, containing 2.20% Pt and 16.3% BaO on a γ-alumina washcoat ($0.11\,g/cm^3$) support adsorbed on a cordierite structure (~ 62 channels/cm^2). Larger cylindrical cores ($D = 3.8$ cm, $L = 7.6$ cm) were cut using a dry diamond saw to a smaller cylindrical shape (ca. $D = 0.8$ cm, $L = 2$ cm, $m_{wc} \sim 0.11$ g). The smaller monoliths were then wrapped in Fiberfrax® ceramic paper and placed in a quartz tube flow reactor. In the results reported below, we differentiate between fresh, aged, and deactivated catalysts, as well as two different catalyst samples. The two different catalyst samples used in this paper were cut from the same original core with approximately identical dimensions, but may have slight variations and are called C1 and C2. We define the "fresh" monolith sample as one with not more than ca. 170 h of operating life. The "aged" monolith sample showed repeatable time-averaged NO_X conversion levels over a wide range of feed compositions. Neither sample was exposed to temperatures exceeding 600 °C since this can lead to rapid deactivation. We have found that the deactivated catalysts exhibited poor NO_X conversion, even under rich conditions.

The experimental set-up used in shown in Fig. 1. The gas delivery system utilized a series of gases and several

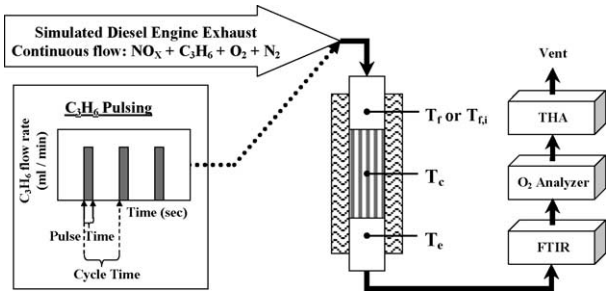

Fig. 1. Schematic representation of the experimental set-up.

mass flow controllers (MFC) to simulate lean exhaust conditions. The current study combined a feed mixture of NO, O_2, and C_3H_6 in a nitrogen carrier; inclusion of CO_2 and H_2O will be investigated in a future study. The flow rates of the gases were controlled with precision mass flow controllers (MKS Inc.). A PC, and ADAM 5000 TCP module (Advantech), and Labtech® software were used for MFC programming and data acquisition. Except as noted, the total gas flow rate was kept constant at 1000 sccm, and individual reactive gas concentrations were varied by adjusting their respective flow rates. The gases were mixed using an in-line static mixer, and then passed through the quartz tube flow reactor positioned inside a Mellen SC11 tube furnace. The reactor temperature was monitored with three K-type thermocouples. The first thermocouple, placed 0.5 cm upstream of the monolith, measured the point gas feed temperature, denoted by T_f. The feed temperature was moderately affected by heat generated by combustion. We therefore distinguish between T_f and $T_{f,i}$, the inert feed temperature, which was measured for a given furnace set point and flow rate while flowing nitrogen through the monolith. The second thermocouple, positioned within an internal monolith channel at the approximate mid-point of the monolith (radial and axial), measured the catalyst temperature (T_c), while the third, positioned 0.5 cm downstream of the monolith, measured the effluent temperature (T_e). These temperatures were continually monitored and recorded. The reactor outlet gases flowed through heated lines (110 °C) to a gas phase system including a FTIR spectrometer, O_2 analyzer and THC analyzer (Total Hydrocarbon Analyzer), as described by Muncrief et al. [11]. The FTIR composition data was collected on a separate PC from the other analyzers and MFCs. The transient data from the different devices were reconciled to account for time delays incurred by flow and response times, including those of the thermocouples, O_2 analyzer, THC, and FTIR [22].

Catalyst storage property measurements were carried out by monitoring the NO_X uptake as a function of the feed temperature, flow rate, and exposure time. In a typical storage experiment, a mixture of 5% O_2 and 500 ppm NO was fed over the catalyst until the NO_X effluent concentration was within 2% of its feed value. NO_X storage was measured over

a prescribed exposure time. The calculated NO_X storage is defined as

$$NO_X \text{ stored} = \frac{\int_0^{t^*} [F_{NO}^0 - F_{NO_X}(t)]\,dt}{m_{catalyst}} \quad (1)$$

where t^* is the exposure time, F_{NO}^0 the feed rate of NO, and F_{NO_X} the effluent molar flow rate of NO_X. The total NO_X uptake measurement was then confirmed by desorbing NO_X from the catalyst using a temperature ramp to 550 °C and quantifying the total NO_X desorbed. After NO_X desorption, propylene pulses diluted in N_2 were injected at 550 °C. The propylene was used as a tracer to determine the time delay between the NO_X injection and breakthrough.

The feed composition was characterized by the stoichiometric number, S_N, defined as the molar ratio of the oxidizing to the reducing components:

$$S_N = \frac{2[O_2] + [NO]}{9[C_3H_6]} \quad (2)$$

The term $S_{N,SS}$ or $S_{N,Avg}$ is used to denote steady-state or time-averaged feed compositions, respectively. $S_{N,Pulse}$ ($S_{N,Lean}$) is used when calculations are based upon only the feed composition during the propylene pulse (lean feed). NO_X conversion is defined by the NO_X reacted ($NO_X = NO + NO_2$) normalized by the NO_X fed. Selectivity to N_2 was determined as the ratio between the amount of NO_X reduced to N_2 and the total amount of NO_X reacted. Since N_2 was not measured directly, we determined the NO_X converted to N_2 as the difference between the total NO_X converted and that converted to N_2O: ($[NO_X]_{reduced}$ to $N_2 = [NO_X]_{reacted} - 2[N_2O]_{formed}$).

Steady-state experiments were carried out to determine the dependence of NO_X conversion on various operating parameters including feed temperature and composition. Steady-state conversion data was obtained by setting the desired feed temperature, and then feeding a prescribed amount of NO, O_2, and reductant to the reactor until the NO_X outlet was time invariant.

For the lean/rich cycling experiments, the lean gas feed mixture composition typically used was 500 ppm NO, 5% O_2, and 1000 ppm C_3H_6 in a balance of nitrogen. During the rich period, C_3H_6 was added at a prescribed flow rate and feed duration. A constant total flow rate was maintained by adjusting the N_2 flow rate. Oxygen and NO flows were maintained constant to simulate the injection of a reductant into a diesel engine exhaust. The independent variables included feed temperature, reductant feed concentration, total cycle time, reductant duty cycle (percentage of total cycle with reductant feed), NO feed concentration, and space velocity (GHSV, h^{-1}, at 25 °C and 1 atm). Most time-averaged data were obtained over at least five cycles, ensuring that the system had reached a pseudo-steady state. The catalytic activity was periodically checked by repeating the experimental conditions of NO_X conversion versus $S_{N,Pulse}$ at an inert feed temperature of 300 °C.

3. Results

3.1. Steady-state NO_X reduction

The steady-state performance of the catalyst was examined over a range of feed compositions spanning rich ($S_{N,SS} < 1$) to lean ($S_{N,SS} > 1$). Fig. 2a shows the NO_X conversion as a function of the stoichiometric number for an inert feed temperature of 300 °C, space velocity of 60,000 h^{-1}, and feed gas containing 500 ppm NO and 5% O_2. The steady-state NO_X conversion approached 20% for lean mixtures and 100% for rich mixtures. A sharp conversion change was observed at a stoichiometric number of unity, the transition between rich and lean. Since the O_2 concentration was fixed at 5%, an increase in propylene concentration (decrease in $S_{N,SS}$) resulted in a monotonic increase in monolith temperature due to the exothermic catalytic oxidation of propylene.

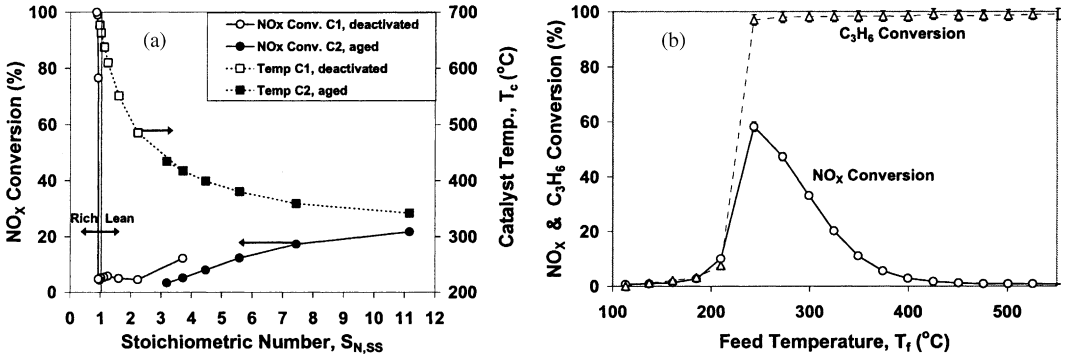

Fig. 2. Steady-state results for a flow composition of 500 ppm NO, 5% O_2, and varying C_3H_6. (a) Steady-state NO_X conversion (○, ●) and catalyst temperature (□, ■) vs. $S_{N,SS}$ at $T_f = 300$ °C. Open symbols are deactivated Cl catalyst, closed symbols are aged C2 catalyst. (b) Steady-state NO_X conversion (○) and C_3H_6 conversion (△) vs. T_c using fresh C1 catalyst and $S_{N,SS} = 11.2$ (1000 ppm C_3H_6).

The effect of feed temperature on NO_X conversion is shown in Fig. 2b for a lean feed mixture ($S_{N,SS} = 11.2$; 0.1% C_3H_6). Light-off occurred at approximately 210 °C, leading to a sharp increase in NO_X and propylene conversion. The lean feed exhibited a peak NO_X conversion (ca. 60%) between 210 and 250 °C. Although the data is not shown, The NO_X selectivity to N_2 was low under extremely lean conditions (ca. 45% at $S_{N,SS} = 11.2$). As the propylene concentration was increased, the selectivity monotonically increased. The point at which 100% selectivity was achieved depended upon the age of the catalyst. The aged catalyst achieved 100% selectivity at $S_{N,SS}$ ca. 3.2, while the deactivated catalyst approached 100% selectivity at $S_{N,SS}$ ca. 1.6.

3.2. NO_X storage and capacity

In order to better understand the effect of catalyst temperature on the NO_X storage rate, we measured the NO_X storage as a function of exposure time (or lean storage time). Fig. 3 shows data for both fresh and aged catalysts. The NO_X storage achieved a maximum value at an intermediate temperature for a fixed exposure time, although the maximum was more pronounced at longer times. For shorter exposure times the NO_X storage was nearly independent of temperature (broad maximum) for a wide range of temperatures. The fresh catalyst stored considerably more NO_X at longer storage times but the effect of aging was less significant at shorter storage times.

3.3. NO_X storage and reduction cycling

A series of cycling experiment were carried out by varying the propylene concentration in a pulse of fixed duty and overall cycle time. Fig. 4 shows four periods of a typical cycling experiment. For this particular experiment, the lean gas feed mixture was kept constant at 500 ppm NO, 5% O_2, and 1000 ppm C_3H_6 with balance N_2. The propylene inlet concentration during the rich phase was 1.4% ($S_{N,Pulse} \sim 0.8$). The total cycle time was 70, 60 s lean and 10 s rich, and the inert feed temperature was 300 °C. During the "lean" period of the cycle, the NO_X was adsorbed (trapped) by the

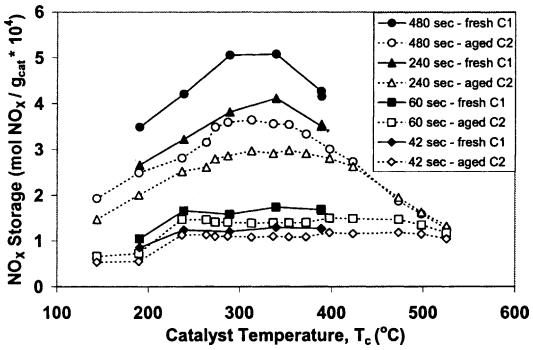

Fig. 3. NO_X storage vs. catalyst temperature (T_c) at several exposure times for fresh C1 and aged C2 catalysts.

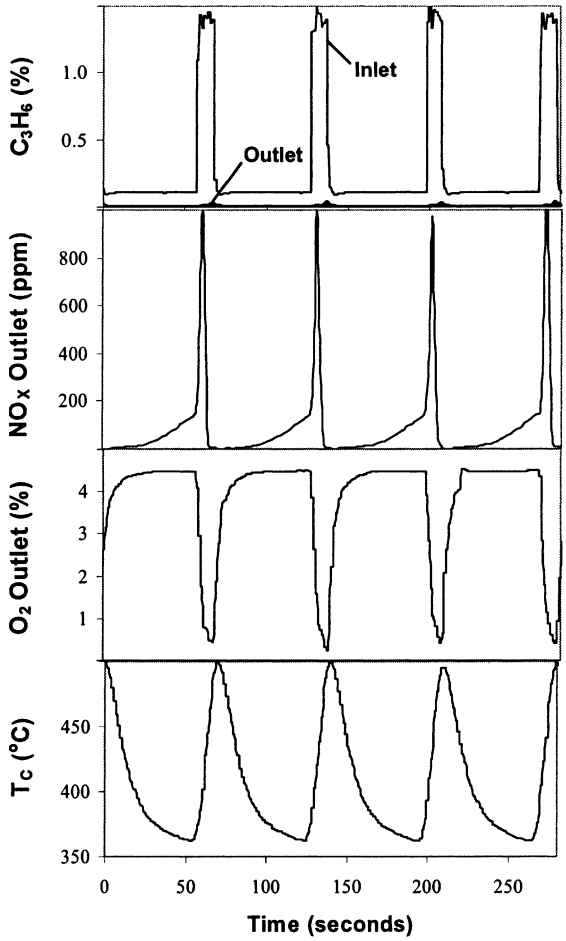

Fig. 4. Transient data during 10 s rich/60 s lean cycling for fresh C2 catalyst. Lean feed composition: 500 ppm NO, 5% O_2, and 1000 ppm C_3H_6. Rich feed composition: 500 ppm NO, 5% O_2, and 1.4% C_3H_6; $T_{f,i} = 300$ °C.

catalyst. As the storage sites were filled, NO_X breakthrough commenced. The reductant (propylene), which was injected during the "rich" period, effected the release and reduction of the surface nitrites/nitrates. The sharp drop in oxygen concentration and corresponding increase in CO_2 and H_2O concentrations and catalyst temperature during the rich period indicated the catalytic oxidation of propylene. During the oxidation, a short excursion in effluent NO_X ($NO + NO_2$) occurred, followed by a sharp decrease to near zero. Once the majority of the oxygen was consumed, small amounts of propylene and CO were observed near the end of the rich cycle. Minor concentrations of N_2O were observed in this experiment.

Fig. 5a illustrates the benefit of intermittent propylene injection. The cycling data correspond to a lean feed mixture of 500 ppm NO, 5% O_2, 1000 ppm C_3H_6, balance N_2, and inert feed temperature at 300 °C. The cycling had the same timing characteristics as in Fig. 4. The propylene feed rate was varied during the pulse to access a wide range of pulse feed compositions. As $S_{N,Pulse}$ decreased from 2.8 towards unity (corresponding to an increase in propylene concen-

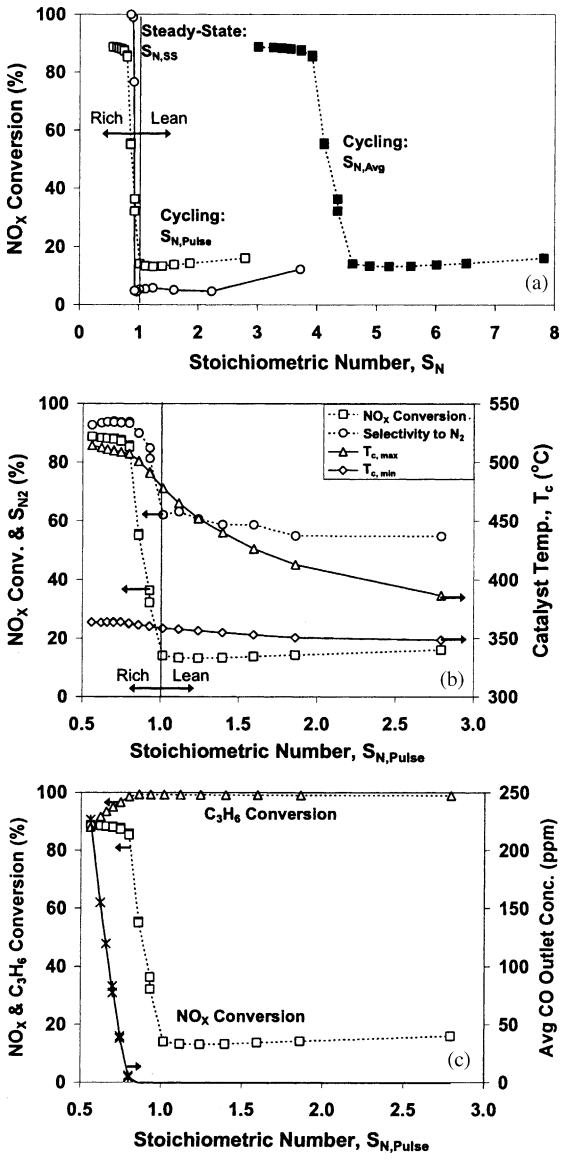

Fig. 5. Time-averaged NO_X conversion vs. S_N for 60/10 lean/rich pulsing experiments using C1 catalyst with a continuous feed of 500 ppm NO, 5% O_2, and 1000 ppm C_3H_6. Additional C_3H_6 is pulsed in during the rich phase; $T_{f,i} = 300\,^{\circ}C$. (a) Comparison of $S_{N,Pulse}$ (□), and $S_{N,Avg}$ (■) to steady-state results (○) shown in Fig. 2. (b) Maximum and minimum catalyst temperature and N_2O selectivity vs. $S_{N,Pulse}$. (c) Propylene conversion and CO breakthrough vs. $S_{N,Pulse}$.

tration from 0.4 to 1.1%) the NO_X conversion slightly decreased. A sharp increase in time-averaged NO_X conversion was observed when the propylene pulse concentration exceeded 1.25% ($S_{N,Pulse} < 0.9$; $S_{N,Avg} < 4.2$). For comparison, under steady-state conditions, a feed consisting of 0.3% propylene ($S_{N,SS} = 3.7$) with NO, O_2, and N_2 at the same levels in the cycling experiments resulted in a steady-state NO_X conversion of only 12%. During the cyclic operation, as the stoichiometric number was reduced, the difference between the maximum and minimum catalyst temperature during the cycle increased (Fig. 5b). Accompanying this trend was an increase in the propylene and CO breakthrough due to incomplete oxidation (Fig. 5c).

The time-averaged NO_X conversion for the fresh C2 catalyst is reported as a function of temperature and operation mode (steady state versus cycling) in Fig. 6a. The cycling data correspond to a lean feed mixture of 500 ppm NO, 5% O_2, 1000 ppm C_3H_6 and balance N_2 ($S_{N,Lean} = 11.1$) and a rich feed mixture of 500 ppm NO, 5% O_2, 1.4% C_3H_6 and balance N_2 ($S_{N,Pulse} = 0.8$). The total cycle time and rich pulse time were fixed at 70 and 10 s, respectively, yielding a time-averaged stoichiometric number ($S_{N,Avg}$) of 3.9. Two corresponding sets of steady-state data are provided, one for lean conditions ($S_{N,SS} = 3.9$, 0.3% C_3H_6) and the other for rich conditions ($S_{N,SS} = 0.8$, 1.4% C_3H_6). The lean, rich, and cycling data all exhibit a sharp increase in conversion at light-off (ca. 225 °C). The lean feed shows a peak steady-state NO_X conversion of approximately 38% at 270 °C feed temperature, whereas the rich feed resulted in nearly complete NO_X conversion over the entire temperature range exceeding 225 °C. The cycling data show a peak NO_X conversion of approximately 94% at 270 °C feed temperature. Although the data is not shown here, the NO_X selectivity to N_2 increased monotonically from ca. 80 to 100% as the feed temperature was increased from 270 to 400 °C under cycling conditions. Fig. 6b shows the time traces for two particular cycling points at different feed temperatures (270 and 400 °C). The time traces at the higher feed temperature reveal a proportionately higher catalyst temperature and higher NO_X breakthrough concentrations throughout the cycle, consistent with the lower time-averaged NO_X conversion.

The dependence of time-averaged NO_X conversion as a function of total cycle time is shown in Fig. 7a. In this experiment, the total cycle time was varied while the following variables were fixed: lean feed composition (500 ppm NO, 5% O_2, 1000 ppm C_3H_6, balance N_2), inert feed temperature (250 °C), rich duty cycle (14%), and rich pulse composition ($S_{N,Pulse} = 0.8$). The maximum conversion (95%) was achieved at a cycle time of about 50 s. At very short cycle times and long cycle times, the conversion dropped to 30 and 70%, respectively. Fig. 7b reports the dependence of the NO_X selectivity to N_2 as a function of total cycle time. The trend is similar to that of the NO_X conversion. The cycle time yielding the highest selectivity (ca. 85%) was 50 s. At very short cycle times and long cycle times, the selectivity dropped to 52 and 67%, respectively.

In order to isolate the effect of pulsing from the pulse composition, several experiments were carried out in which the total propylene (moles injected) was fixed but the duty cycle was varied (Fig. 8). The lean feed composition and inert feed temperature were fixed at 500 ppm NO, 5% O_2, 1000 ppm C_3H_6, balance N_2 and 300 °C, respectively. The total cycle time and pulse volume of propylene were fixed at 49 s and 2.3 standard ml, respectively. The choice of the cycle time was dictated by the maximum NO_X conversion achieved in the cycle time study (Fig. 7a). The hydrocarbon

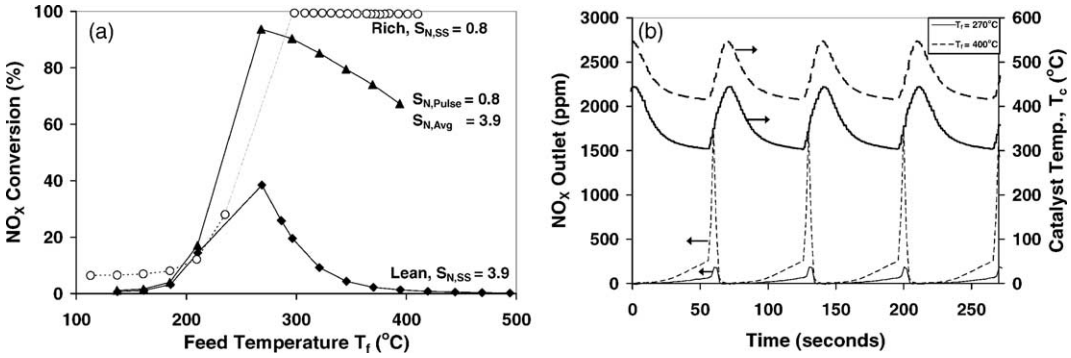

Fig. 6. Steady-state and transient time-averaged NO_X conversion vs. feed temperature (T_f) for fresh C2 catalyst. (a) NO_X conversion vs. feed temperature, T_f. (b) Time trace of NO_X and monolith temperature for 270 and 400 °C average feed temperature (T_f). Lean fed composition: 500 ppm NO, 5% O_2, and 1000 ppm C_3H_6. Rich feed composition: 500 ppm NO, 5% O_2, and 1.4% C_3H_6.

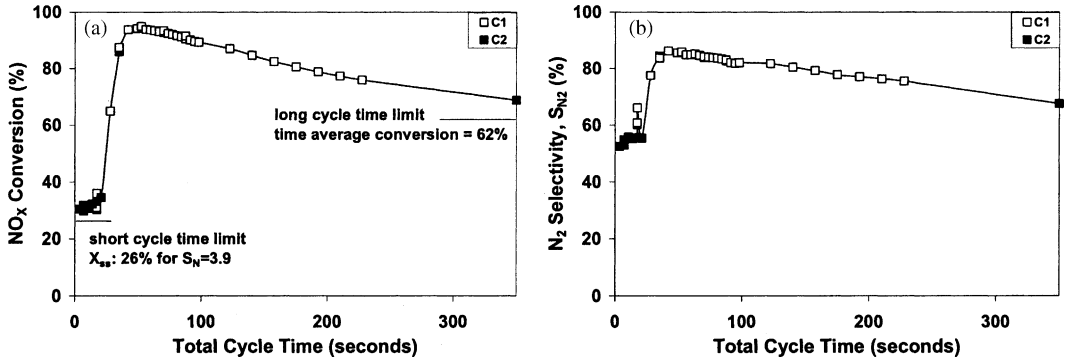

Fig. 7. (a) Time-averaged NO_X conversion vs. total cycle time: $T_{f,i} = 250$ °C, fixed 14% DCR, 1.4% C_3H_6 during rich pulse for fresh C1 and C2 catalysts. (b) N_2 selectivity vs. total cycle time.

pulses ranged from short, very rich pulses, to long, less concentrated pulses. The results in Fig. 8a (expanded view in Fig. 8b) reveal a significant increase in NO_X conversion as the pulse intensity increased, indicating that short, rich pulses are more effective than longer, leaner pulses. The time-averaged propylene breakthrough (conversion) increased (decreased) as the duty cycle decreased. Significant changes in the NO_X and propylene conversion occurred when the pulse became rich ($S_{N,Pulse} < 1$). The trend in N_2 selectivity is similar to that of NO_X conversion, indicating a similar maximum at an intermediate percentage duty cycle rich (Fig. 8c).

The time-averaged NO_X conversion is reported as a function of gas hourly space velocity in Fig. 9a. In this set of experiments the lean feed composition consisted of 500 ppm NO, 5% O_2, 1000 ppm C_3H_6 and balance N_2. Propylene concentration in the pulse was varied over a wide range, with the cycle time fixed at 70 s, rich pulse time fixed at 10 s, and the inert feed temperature fixed at 300 °C. Under lean conditions ($S_{N,Pulse} > 1$) higher space velocities resulted in higher NO_X conversions due to a reduction in the time-averaged catalyst temperature. Similar to previous results, as the propylene concentration was increased above 1.25% ($S_{N,Pulse} < 0.9$), a sharp increase in time-averaged NO_X conversion occurred. Fig. 9b shows N_2 selectivity data as a function of GHSV and $S_{N,Pulse}$. We define the reactor volumetric productivity, P_{NO_X}, as

$$P_{NO_X}\left(\frac{\text{mol NO}_X \rightarrow \text{N}_2}{\text{l}_{\text{monolith}}\text{h}}\right) = \frac{F^0_{NO_X}(\text{mol NO}_X \text{ fed/h})\, X_{NO_X}(\text{mol NO}_X \text{ reacted/mol NO}_X \text{ fed})\, S_{N_2}(\text{mol NO}_X \rightarrow \text{N}_2/\text{mol NO}_X \text{ reacted})}{V(\text{l}_{\text{monolith}})} \quad (3)$$

P_{NO_X} is effectively a space–time yield of N_2. Fig. 9c shows the dependence of P_{NO_X} as a function of $S_{N,Pulse}$. The results show that a higher space velocity results in a higher productivity, independent of the operating regime (rich or lean). The corresponding temperature dependencies on $S_{N,Pulse}$ are shown in Fig. 9d. As seen earlier in Fig. 5b, when the stoichiometric number is reduced during the cyclic operation, the difference between the maximum and minimum catalyst temperature during the cycle increases. This temperature difference widens as the space velocity increases.

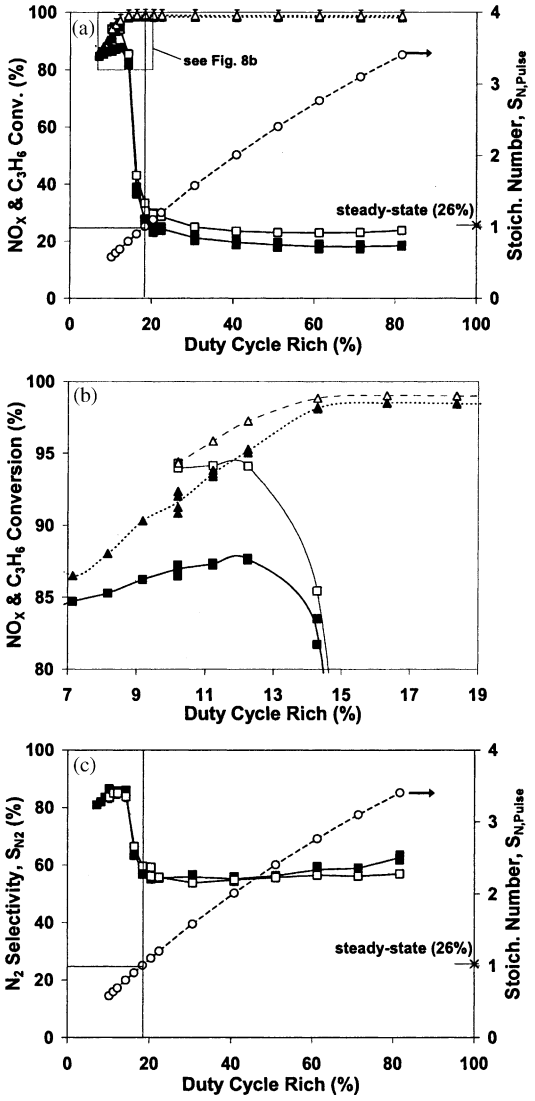

Fig. 8. (a) NO_X conversion (—) and propylene conversion (- - -) vs. rich duty cycle for fresh C1 (□) and aged C2 (■) catalysts: $T_{f,i} = 250\,^{\circ}C$, 49 s total cycle time, fixed total mol C_3H_6 injected. (b) Enlarged inset from part (a). (c) N_2 selectivity (—) vs. rich duty cycle for fresh C1 (□) and aged C2 (■) catalysts.

Selected time traces for the $S_{N,Pulse} = 0.8$ experiment are provided in Fig. 10 in order to elucidate the effect of space velocity. As noted before, the NO_X adsorbs onto the catalyst during the "lean" period and desorbs during the "rich" period. A brief NO_X excursion occurs immediately after the propylene injection, followed by a sharp decrease (Fig. 10a). Whereas the NO_X excursions are more pronounced for lower space velocities, the NO_X effluent concentration is lower during the lean period. Fig. 10b shows that propylene breakthrough commences near the end of the rich cycle. The space velocity has only a minor effect on the C_3H_6 breakthrough and N_2O production. Fig. 10c shows the temperature transients during cycling at the various space velocities (at $S_{N,Pulse} = 0.8$). For higher space velocities, a cooler catalyst temperature is maintained during the lean period, while a hotter catalyst temperature is achieved during the rich period. Fig. 10d compares the NO_X stored and reacted over the cycle at the different space velocities. Although Fig. 10a shows that more NO_X breaks through during the lean period at higher space velocities, Fig. 10d shows that more NO_X is also stored on the catalyst during this period.

4. Discussion

A comprehensive study has been carried out for NO_X storage and reduction in a model monolith reactor containing a $Pt/BaO/Al_2O_3$ washcoated catalyst. Our findings indicate that periodic operation of the lean/rich selective catalytic reduction process results in enhanced NO_X conversion, in agreement with recent studies [11,15,23,24]. The combination of NO_X storage/trapping and intermittent pulsing of a reductant gives NO_X conversions that significantly exceed those obtained under steady-state conditions.

The steady-state results are typical of lean SCR with propylene on Pt (Figs. 2 and 6). Ignition occurs at about 225 °C, leading to essentially complete conversion of propylene. Corresponding with the depletion of propylene is a maximum in the NO_X conversion (60%) at a feed (catalyst) temperature of 240 °C (285 °C) for $S_{N,SS} = 11.2$. The NO_X conversion drops sharply with further increases in temperature. This is attributed to the combined effect of oxygen inhibition of NO adsorption and dissociation and enhanced NO desorption at higher temperatures [25,26]. The high NO_X conversion under rich conditions using propylene as a reductant has been reported by others [19,27].

The NO_X storage dependence on temperature reflects the contribution of kinetic and thermodynamic factors (Fig. 3). These uptake data exhibit a maximum at an intermediate temperature, as reported in previous studies [12,13,15]. The increase in NO_X storage with exposure time at a fixed temperature is clearly in a kinetic regime. The uptake rate is controlled by NO_X sorption to one or more site types [21,28], the NO_X feed rate [21], and/or by NO diffusion through a barium nitrate layer to an underlying oxide or carbonate layer [23]. The storage maximum, which is more pronounced at longer exposure times, conveys the transition between kinetic and thermodynamic limitations. To the left of the maximum the storage increases with temperature, indicative of a kinetic limitation. To the right of the maximum the storage decreases with temperature due to the onset of the reversible decomposition of the nitrate [29,30]. Further evidence for the equilibrium limitation is the fact that the storage becomes independent of exposure time at very high temperatures (>500 °C). It is interesting to note that very broad maximum at the shorter exposure times. Here the storage is nearly independent of temperature, which indicates a mass transport limitation, which would be expected to be a weak function of temperature.

A temporal analysis under lean–rich cycling reveals several notable features of the NO_X storage and release and propylene oxidation (Fig. 4). Several characteristic periods

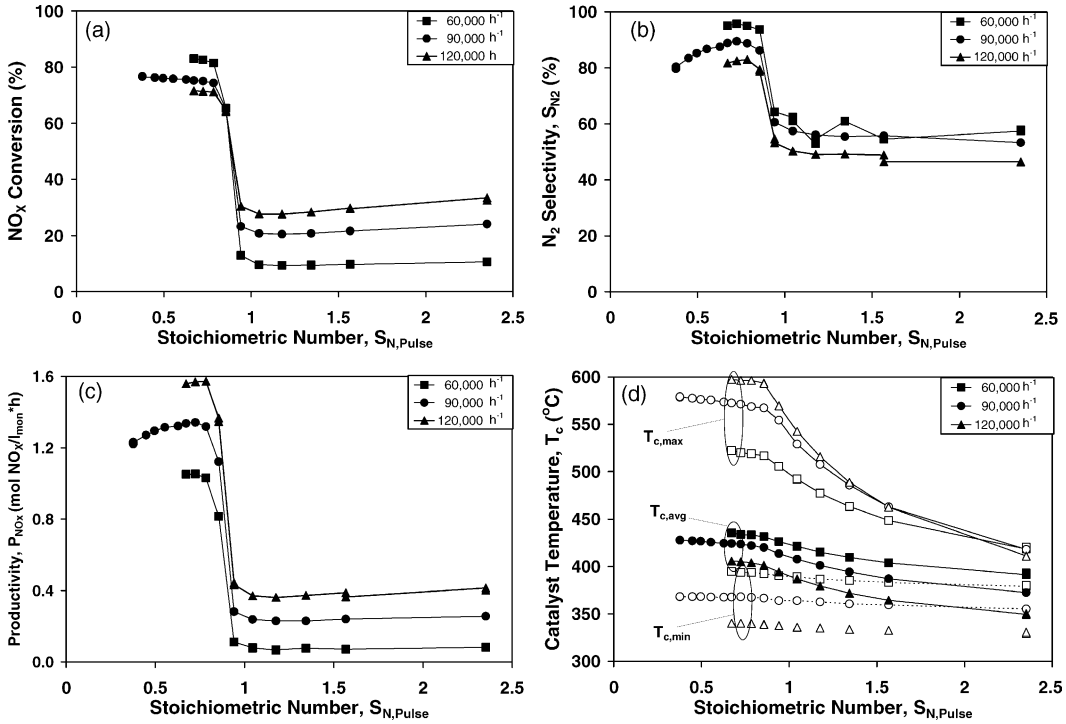

Fig. 9. Lean feed composition: 500 ppm NO, 5% O_2, and 1000 ppm C_3H_6. Additional C_3H_6 is pulsed in during the rich phase: $T_{f,i} = 300\,^{\circ}C$, 60 s lean/10 s rich, aged C2 catalyst; GSHV varied. (a) NO_X conversion vs. $S_{N,Pulse}$; (b) N_2 selectivity vs. $S_{N,Pulse}$; (c) productivity vs. $S_{N,Pulse}$; (d) catalyst temperature vs. $S_{N,Pulse}$.

are evident in the NO_X breakthrough consistent with reports by others of the complete NO_X storage and reduction cycle [11,15]. A period of complete NO_X storage without breakthrough is followed by a slow increase in the effluent NO_X. For the case shown in Fig. 4, these periods last approximately 20 and 40 s, respectively. When propylene is injected there is a large jump in the effluent NO_X concentration. This NO_X release with incomplete NO_X reduction

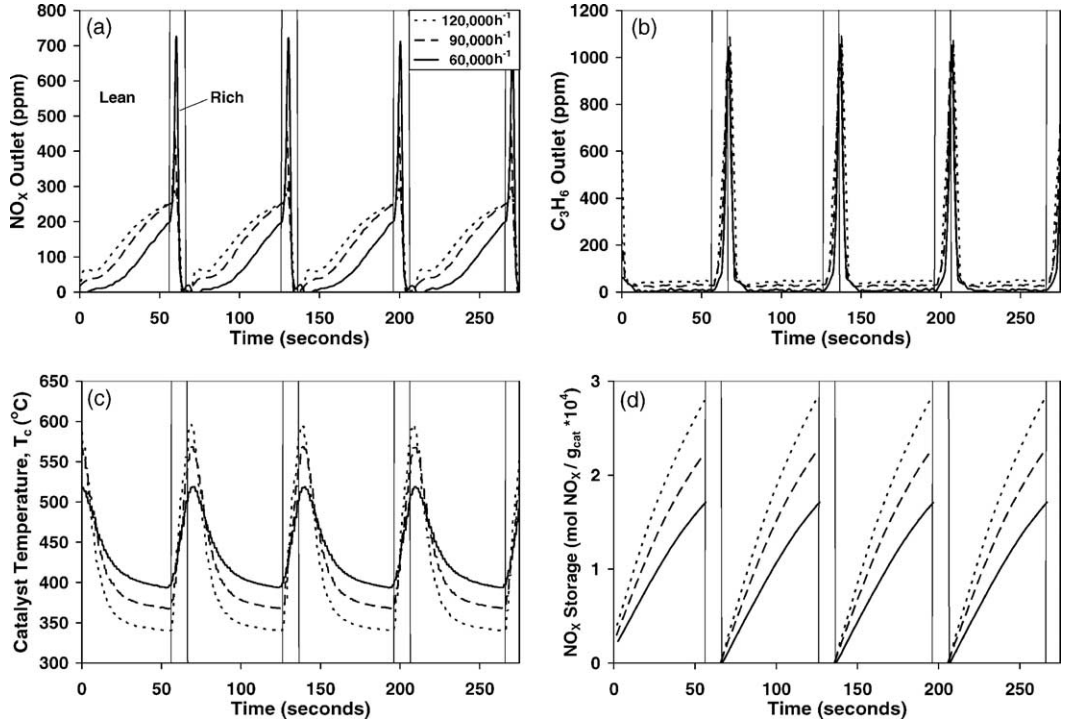

Fig. 10. Transient data for several GHSV values for aged C2 catalyst. Same conditions as in Fig. 9.

is not completely understood, but is attributed in part to the exotherm generated by the oxidation reaction and the balancing of the competing adsorptions of NO_X and propylene on Pt sites [15,16,31]. The measured monolith temperature rise is about 135 °C for this particular experiment, resulting in a peak catalyst temperature of 500 °C. As shown in the storage results (Fig. 3), temperatures exceeding 500 °C lead to the decomposition of barium nitrate. For a short period of about 10 s considerable NO and NO_2 breakthrough occurs, with the maximum NO_X effluent concentration (ca. 1000 ppm) well in excess of the feed concentration (500 ppm). But this breakthrough is short-lived, as a sharp drop in the effluent NO_X then occurs. Expectedly, the effluent oxygen decreases after the propylene injection due to propylene oxidation. The switch to net rich conditions with incomplete propylene conversion is favorable for NO_X reduction. As the steady-state results showed (Fig. 6), the NO_X conversion approaches 100% under rich conditions and temperatures exceeding 300 °C. Previous steady-state studies have shown that the NO_X conversion and N_2 selectivity increase with temperature under rich conditions [32,33].

The propylene concentration during the pulse is a critical parameter affecting NO_X trap performance. The results in Fig. 5 show that the propylene pulse must be rich ($S_{N,Pulse} < 1$) in order to achieve high NO_X conversion. A sharp jump in the time-averaged NO_X conversion occurs as the pulse just becomes rich ($S_{N,Pulse} = 0.9$). The increase corresponds closely to that obtained under steady-state conditions. These findings are in agreement with our previous results with Pt/BaO/alumina powder [11]. An increased propylene concentration also increases the N_2 selectivity (reduces N_2O selectivity) from ca. 50% for $S_{N,Pulse} > 1$ to greater than 90% or $S_{N,Pulse} < 0.75$. The selectivity increase is attributed to the higher monolith temperatures achieved as the propylene pulse concentration is increased; i.e. the temperature excursions benefit the selective catalytic reduction of NO.

The periodic pulsing of propylene has a dramatic enhancement effect on the NO_X conversion. As Fig. 5a shows, for example, a steady-state feed containing 0.37% propylene ($S_{N,SS} = 3$) gives a NO_X conversion of about 10%. If an equivalent amount of propylene is fed during a pulse of sufficiently short duration, such that the pulse is fuel-rich, the conversion approaches 90%. This is in spite of the reactor operating in a net oxidizing atmosphere for most of the cycle (Fig. 4). This suggests that during the period of oxygen deficiency selective reduction of NO_X occurs, with a rate enhanced by the higher temperature resulting from the oxidation of propylene. Olsson et al. [31] have proposed that reaction occurs between stored NO_X and CH_2 adsorbed on Pt, releasing NO. The formation of N_2 is proposed to occur by conventional selective catalytic reduction on Pt which predominates during the oxygen deficient period. It seems plausible that selective catalytic reduction may continue even after the rich pulse period with NO_2 competing with O_2 for residual hydrocarbon fragments on the surface. Additional studies are needed to elucidate the causative steps leading to the conversion enhancement.

While the conversion enhancement is attained over a relatively wide range of operating conditions, the results show that superior results require a tuned cycle protocol in terms of storage time, pulse duration and composition, and feed temperature. The decrease in time-averaged conversion at higher feed temperature, as shown in Fig. 6a, is attributed to the combination of reduced NO_X storage capacity and NO_X release without reduction during the rich pulse. We have shown that the catalyst temperature exhibits large excursions during cycling. For example, operation at the inert feed temperature of 300 °C for 70 s cycle time ($S_{N,Pulse} = 0.85$) results in catalyst temperatures between 360 and 500 °C, with a time-averaged value of 406 °C (Fig. 5b). As shown in Fig. 3, temperatures exceeding 500 °C lead to reduced NO_X storage, even for the 42 s lean period. As shown by Theis et al., the NO_X release during the rich pulse is a sensitive function of temperature [15]. This is apparent in Fig. 6b, which compares the NO_X effluent for average feed temperatures of 270 and 400 °C.

The NO_X conversion is maximized at an intermediate cycle time and rich duty fraction. These monolith reactor results are in general agreement with results found previously for powder catalyst [11]. As shown in Figs. 7 and 8, the NO_X conversion achieves a maximum conversion between 85 and 95% at a cycle time of about 50 s as long as the propylene pulse is sufficiently intense (i.e. short in duration, high in concentration). The conversion approaches the limiting values of about 25 and 60% as the cycle time is decreased to <20 and >300 s, respectively (Fig. 7a). As discussed previously by Muncrief et al. [11], the short cycle time limit corresponds to the conversion achieved for a well-mixed feed. Dilution due to dispersion of the reactor feed contributes to the conversion decrease. On the other hand, at very short cycle times the catalyst is not be able to respond quickly enough to the time-varying feed with the outcome being a conversion level corresponding to that of a mixed feed. We have confirmed this in a modeling study to be reported elsewhere. The long cycle time limit is essentially a weighted-average of the rich and lean steady-state conversion. Finally, variation of the duty cycle with the cycle time fixed at 49 s indicates that short pulses are beneficial to a point (Fig. 8a). The large jump in conversion as the pulse duty fraction is decreased corresponds to the pulse becoming rich (Fig. 8c). This agrees with other results (Fig. 5).

An adverse result of intensifying the propylene pulse is an increased breakthrough of unconverted propylene. The results from fresh and aged monolith catalyst reveal a large increase in the effluent propylene as the pulse duty cycle is decreased (Fig. 8b). This result, together with evidence for a maximum in the NO_X conversion (Fig. 8a), implies that there is an optimal pulse duration and propylene concentration; i.e. one giving maximal conversion of NO_X and minimal breakthrough of propylene. If the feed pulse is too intense, the monolith is unable to completely oxidize the propylene

due in part to the temporal depletion of oxygen. Evidence for the decrease in NO_X conversion when the pulse duty is reduced below 12% (Fig. 8b) suggests the onset of a different mechanism. The existence of the NO_X conversion maximum may suggest inhibition of NO_X adsorption by carbonaceous species and CO on Pt sites.

The dependence of the time-averaged NO_X conversion on the space velocity exhibits an inversion at the rich-lean boundary ($S_{N,Pulse} = 1$), as shown in Fig. 9. In the lean-pulse regime ($S_{N,Pulse} > 1$) the conversion increases with increasing space velocity whereas it decreases in the rich pulse regime ($S_{N,Pulse} > 1$). The conversion trends in the lean regime are attributed to a nonisothermal kinetic effect. As the monolith temperature data in Fig. 9d reveal, higher flow rates reduce the time-averaged temperature. We have already seen that lower catalyst temperature under steady-state conditions leads to increased NO_X conversion (Fig. 2a), a trend attributed to kinetic factors. This reasoning is expected to hold under cycling conditions because propylene conversion is nearly complete and oxygen, which remains in excess the entire cycle, blocks sites for NO adsorption and reduction.

In order to interpret the NO_X conversion results in the rich regime, we must consider the effect of space velocity on reactant supply and NO_X storage. An increase in space velocity for a fixed NO feed concentration increases the amount of NO_X contacting the catalyst for a fixed exposure time. This is similar to increasing the exposure time at a fixed flow rate (Fig. 3). Those data revealed an increase in the NO_X storage with exposure time. Similarly, an increase in space velocity for a fixed rich pulse time increases the supply of propylene over the course of an entire lean–rich cycle.

These effects, coupled with nonisothermal effects, help to explain the data in Fig. 9. Basically, higher space velocity conditions give superior thermal conditions for NO_X storage and reduction. One needs to examine the subtle details of the temporal temperature dependence to support this point. Monolith temperature data show that the gap between the maximum and minimum catalyst temperatures during a cycle widens with increasing space velocity (Fig. 9d). Specifically, for a fixed feed composition (S_N), the peak temperature increases whereas the minimum temperature decreases. The wider swing in temperature at the higher space velocity indicates a higher rate of propylene oxidation and therefore heat generation during the rich pulse (note that the propylene conversion is essentially complete and independent of space velocity, Fig. 10b) and a more rapid cooling during the lean period. Fig. 10c shows the time dependence of the monolith temperature for the three space velocities with the rich pulse fixed at $S_{N,Pulse} = 0.8$. For example, at a space velocity of 120,000 h^{-1} the monolith temperature is below 400 °C for most of the lean period (propylene pulse turned off), whereas the temperature is well above 400 °C the same period at 60,000 h^{-1}. On the other hand, the monolith temperature approaches 600 °C during the rich period at 120,000 h^{-1}, whereas the peak monolith temperature does not exceed 520 °C at the lower space velocity. The combination of a lower storage temperature and higher reduction temperature benefit the NO_X storage and reduction. Moreover, the higher space velocity results in a higher NO_X storage for a fixed duration time (Fig. 10d). As Fig. 9c shows more NO_X is converted per cycle at the higher throughput. Since a doubling in the space velocity does not result in a proportional increase in the space–time yield, the NO_X conversion is lower at the higher space velocity.

The results found in this study suggest that there exists an optimal set of operating conditions that maximize the time-averaged conversion of NO_X. In most of the experiments reported in this study, the total flow rate was fixed at 1 l/min and the NO_X feed concentration was 500 ppm. At these conditions we found that a catalyst temperature of about 350 °C, and a feed protocol consisting of a 50 s cycle and 7 s rich pulse resulted in high NO_X conversion. One would expect that the protocol should vary with the space velocity, among other factors, such as catalyst stability and supplemental fuel requirements. As mentioned above, in the space velocity experiments, the lean–rich protocol of 7 s rich/42 s lean is optimal for a space velocity of 60,000 h^{-1} (Fig. 7a). However, at the higher space velocity (120,000 h^{-1}) a shorter lean period would be needed in order to reduce NO_X breakthrough.

Regarding the important issue of catalyst stability and deactivation, we observed a slow catalyst deactivation with time on stream. The NO_X trap performance degraded more rapidly during excessive temperature excursions (exceeding 600 °C). Jang et al. suggested that at temperatures above 600 °C a Ba–Al solid alloy forms which reduces the sorption capacity by nearly 70% for a powder alumina catalyst containing Ba [20]. At temperatures above 950 °C, a stable $BaAl_2O_4$ compound is formed [20]. Sung and Burk have suggested that the primary deactivation mechanism is the sintering of the Pt [24]. However, Ford researchers reported that sol–gel processed catalysts can withstand temperatures up to 900 °C [34]. Regardless of the mechanism, protocols that avoid such excursions should be followed. This is also a critical issue during catalyst desulfation which is necessary when using sulfur-containing fuels.

5. Conclusions

A comprehensive study of NO_X storage and reduction has been carried out to understand the effect of feed conditions on the performance of a model Pt/BaO/alumina washcoated monolith. The results reveal that periodic pulsing of a reductant to the catalyst containing stored nitrate is an effective approach for addressing the challenge of reducing NO_X in a lean exhaust stream. The results show that significant enhancement in time-averaged NO_X conversion is achieved through intermittent, short pulses of reductant into a stream containing NO_X and excess oxygen. The NO_X conversion achieves a maximum at an intermediate temperature. The

window of high conversion is much wider than that obtained during conventional steady-state selective catalytic reduction of NO_X by hydrocarbons. Finally, the feed protocol must be tuned to achieve a maximum NO_X conversion for a given set of feed conditions.

The results reported in this study considered a feed gas devoid of water, CO_2, and SO_2. As pointed out by Epling et al. [28], all diesel exhaust contains these components so the influence of these species on the NO_X trap performance should be investigated.

The transient performance of the monolithic NO_X trap is quite complex due to the nonlinear kinetics, storage, and nonisothermal effects. A systematic variation of key feed variables is warranted in order to identify regimes of optimal operation. Moreover, dynamic reactor models are needed to guide the NO_X trap optimization efforts. A recent study by Marek and coworkers is a step in the right direction [35,36]. An essential element of predictive models is the development of a kinetic model that captures the transient kinetics, such as the study by Olsson et al. [16,31]. Finally, the fuel type and requirements to achieve a prescribed NO_X conversion is an important consideration. This issue is the subject of current research and will be reported elsewhere.

Acknowledgements

The support of the State of Texas Advanced Technology Program (ATP) is gratefully acknowledged. We also acknowledge fruitful technical discussion with Dr. Yuejin Li of Engelhard Corporation and Dr. Gregor Kolios of the University of Stuttgart.

References

[1] J.C. Frost, G. Smedler, Catal. Today 26 (1995) 207.
[2] J.C. Clerc, Appl. Catal. B: Environ. 10 (1996) 99.
[3] R.J. Farrauto, K.E. Voss, Appl. Catal. B: Environ. 10 (1996) 29.
[4] P.L. Herzog, Stud. Surf. Sci. Catal. 116 (1997) 35.
[5] E.S. Lox, B.H. Engler, E. Koberstein, Stud. Surf. Sci. Catal. 71 (1990) 291.
[6] Diesel Technology Forum, vol. 2003, 2001.
[7] Environmental Protection Agency (EPA), vol. 2003, 2003.
[8] M. Shelef, Chem. Rev. 95 (1995) 209.
[9] W.E.J. van Kooten, H.P.A. Calis, C.M. van den Bleek, Stud. Surf. Sci. Catal. 116 (1997) 357.
[10] J.N. Armor, K. Li, Appl. Catal. B: Environ. 5 (1995) 257.
[11] R.L. Muncrief, K.S. Kabin, M.P. Harold, AIChE J., in press.
[12] E. Fridell, M. Skoglundh, B. Westerberg, S. Johansson, G. Smedler, J. Catal. 183 (1999) 196.
[13] E. Fridell, M. Skoglundh, S. Johansson, B. Westerberg, A. Torncrona, G. Smedler, Stud. Surf. Sci. Catal. 116 (1997) 537.
[14] A. Amberntsson, H. Persson, P. Engstrom, B. Kasemo, Appl. Catal. B: Environ. 31 (2001) 27.
[15] J.R. Theis, J.A. Ura, J.J. Li, G.G. Surnilla, J.M. Roth, C.T.J. Goralski, SAE International, 2003-01-1159, 2003, p. 5.
[16] L. Olsson, H. Persson, E. Fridell, M. Skoglundh, B. Andersson, J. Phys. Chem. B 105 (2001) 6895.
[17] P. Broqvist, I. Panas, E. Fridell, H. Persson, J. Phys. Chem. B 106 (2002) 137.
[18] W. Bogner, M. Kramer, B. Krutzsch, S. Pischinger, D. Voigtlander, G. Wenninger, F. Wirbeleit, M.S. Brogan, R.J. Brisley, D.E. Webster, Appl. Catal. B: Environ. 7 (1995) 153.
[19] P.-H. Han, Y.-K. Lee, S.-M. Han, H.-K. Rhee, Top. Catal. 16–17 (2001) 165.
[20] B.-H. Jang, T.-H. Yeon, H.-S. Han, Y.-K. Park, J.-E. Yie, Catal. Lett. 77 (2001) 21.
[21] H.Y. Huang, R.Q. Long, R.T. Yang, Energy Fuel 15 (2001) 205.
[22] K.S. Kabin, Ph.D. Dissertation, University of Houston, in preparation.
[23] U. Tuttlies, V. Schmeisser, G. Eigenberger, Proceedings of the Sixth Int. Cong. on Catal. and Automot. Poll. Control, Brussels, Belgium, October 22–24, 2003.
[24] S. Sung, P.L. Burk, A high temperature stable lean NO_x trap catalyst for automobile application, Paper No. 550a, San Francisco, November 16–21, 2003.
[25] R. Burch, P.J. Millington, Catal. Today 26 (1995) 185.
[26] D.K. Captain, K.L. Roberts, M.D. Amiridis, Catal. Today 42 (1998) 93.
[27] N. Takahashi, H. Shinjoh, T. Iijima, T. Suzuki, K. Yamazaki, K. Yokota, H. Suzuki, N. Miyoshi, S.I. Matsumoto, T. Tanizawa, T. Tanaka, S.-S. Tateishi, K. Kasahara, Catal. Today 27 (1996) 63.
[28] W.S. Epling, G.C. Campbell, J.E. Parks, Catal. Lett. 90 (2003) 45.
[29] J.A. Anderson, B. Bachiller-Baeza, M. Fernandez-Garcia, Phys. Chem. Chem. Phys. 5 (2003) 4418.
[30] X. Li, M. Meng, P. Lin, Y. Fu, T. Hu, Y. Xie, J. Zhang, Top. Catal. 22 (2003) 111.
[31] L. Olsson, E. Fridell, M. Skoglundh, B. Andersson, Catal. Today 73 (2002) 263.
[32] M. Iwamoto, H. Hamada, Catal. Today 10 (1991) 57.
[33] M. Huuhtanen, T. Kolli, T. Maunula, R.L. Keiski, Catal. Today 75 (2002) 379.
[34] C.K. Narula, S.R. Nakouzi, R. Wu, C.T.J. Goralski, L.F.J. Allard, AIChE J. 47 (2001) 74.
[35] P. Koci, M. Marek, M. Kubicek, T. Maunula, M. Harkonen, Chem. Eng. J. 97 (2004) 131.
[36] P. Koci, M. Kubicek, M. Marek, Chem. Ing. Tech. 74 (2002) 566.